BBA - Proteins and Proteomics 1867 (2019) 359–366

Contents lists available at ScienceDirect

BBA - Proteins and Proteomics

journal homepage: www.elsevier.com/locate/bbapap

In depth, thermodynamic analysis of Ca^{2+} binding to human cardiac troponin C: Extracting buffer-independent binding parameters

Rachel A. Johnson[a], Lindsay M. Fulcher[a], Katie Vang[a], Caitlin D. Palmer[a], Nicholas E. Grossoehme[b], Anne M. Spuches[a,*]

[a] Department of Chemistry, East Carolina University, 300 Science and Technology, Greenville, NC 27858, United States
[b] Department of Chemistry, Physics and Geology, Winthrop University, Rock Hill, SC 29730, United States

ARTICLE INFO

Keywords:
ITC
Thermodynamics
EF-hand proteins
Human cardiac TnC
Calcium binding
Buffer-independent parameters

ABSTRACT

Background: Characterizing the thermodynamic parameters behind metal-biomolecule interactions is fundamental to understanding the roles metal ions play in biology. Isothermal Titration Calorimetry (ITC) is a “gold-standard” for obtaining these data. However, in addition to metal-protein binding, additional equilibria such as metal-buffer interactions must be taken into consideration prior to making meaningful comparisons between metal-binding systems.

Methods: In this study, the thermodynamics of Ca^{2+} binding to three buffers (Bis-Tris, MES, and MOPS) were obtained from Ca^{2+}-EDTA titrations using ITC. These data were used to extract buffer-independent parameters for Ca^{2+} binding to human cardiac troponin C (hcTnC), an EF-hand containing protein required for heart muscle contraction.

Results: The number of protons released upon Ca^{2+} binding to the C– and N-domain of hcTnC were found to be 1.1 and 1.2, respectively. These values permitted determination of buffer-independent thermodynamic parameters of Ca^{2+}-hcTnC binding, and the extracted data agreed well among the buffers tested. Both buffer and *pH*-adjusted parameters were determined for Ca^{2+} binding to the N-domain of hcTnC and revealed that Ca^{2+} binding under aqueous conditions and physiological ionic strength is both thermodynamically favorable and driven by entropy.

Conclusions: Taken together, the consistency of these data between buffer systems and the similarity between theoretical and experimental proton release is indicative of the reliability of the method used and the importance of extracting metal-buffer interactions in these studies.

General significance: The experimental approach described herein is clearly applicable to other metal ions and other EF-hand protein systems.

1. Introduction

Metals play critical structural, enzymatic, and signaling roles in biological systems. As a result, nature has evolved sophisticated mechanisms to maintain metal homeostasis [1,2]. Divalent calcium is one example of a metal ion that acts as a secondary messenger in cells; a function made possible by the ubiquitous intra and extracellular calcium-binding proteins (CaBPs) that operate as Ca^{2+} buffers, transporters, and sensors [3–5]. The largest family of CaBPs contains the EF-hand motif, a 12-amino acid Ca^{2+} binding sequence flanked by two alpha helices. The canonical 12-amino acid Ca^{2+}-binding region presents a pentagonal bipyramidal coordination geometry with direct ligation predominantly from glutamic and aspartic acid side chains with contributions from a backbone carbonyl and one water molecule [6].

One intracellular CaBP that serves a crucial function in the animal kingdom is cardiac troponin C (cTnC), an EF-hand protein that binds Ca^{2+} to initiate muscle contraction in the myocardium [7]. Cardiac troponin C consists of two domains, each containing a pair of EF-hand sequences (Fig. 1A). The C-domain binds two Ca^{2+} ions with positive cooperativity and an affinity of $\sim 10^7$, while the regulatory or N-domain contains two EF-hand motifs but binds only one Ca^{2+} ion (EF-hand II) with an affinity that is two orders of magnitude lower than the C-

---

Abbreviations: CaBP, Calcium-binding protein; cTnC, Cardiac Troponin C; hcTnC, Human Cardiac Troponin C; ITC, Isothermal Titration Calorimetry; NTD, No Thermal Detection; NA, Not applicable; ICP-OES, Inductively Coupled Plasma Optical Emission Spectrometry

* Corresponding author.
E-mail address: spuchesa@ecu.edu (A.M. Spuches).

https://doi.org/10.1016/j.bbapap.2019.01.004
Received 8 August 2018; Received in revised form 28 December 2018; Accepted 6 January 2019

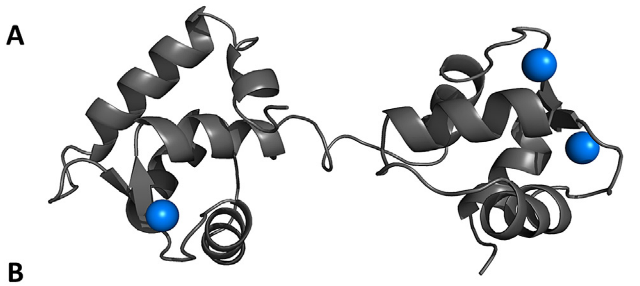

B

		<u>1</u>	2	<u>3</u>	4	<u>5</u>	6	<u>7</u>	8	<u>9</u>	10	11	<u>12</u>
EF Hand I:	-V	L	G	A	E	**D**	**G**	C	**I**	S	T	K	**E**
EF Hand II:	**-D**	E	D	G	S	**G**	T	V	**D**	F	**D**	**E**	
EF Hand III:	**-D**	**K**	**N**	A	**D**	**G**	Y	**I**	**D**	L	**D**	**E**	
EF Hand IV:	**-D**	**K**	**N**	N	**D**	**G**	R	**I**	**D**	Y	**D**	**E**	

Fig. 1. A) NMR solution structure of Ca^{2+} bound N- (Left) and C-domain (Right) of cTnC (PDB ID 1AJ4). B) The 12 and 13 (EF-Hand I) amino acid loop region of EF hands I-IV. Underlined positions (1, 3, 5, 7, 9, and 12) represent location of residues participating in Ca^{2+} ligation. Conserved amino acid residues are in bold. The Asp residue located in position 9 binds Ca^{2+} indirectly via a bridging water molecule. EF-hand I does not bind Ca^{2+} due to the non-polar amino acid substitutions located in postions 1 and 3.

domain [8]. EF-hand I is also known as a "defunct" loop and does not bind Ca^{2+} due to evolved non-polar amino acid substitutions in positions 1 and 3 of loop I (Fig. 1B) [9].

Our understanding of cardiac troponin C and its role in muscle contraction stem from a multitude of spectroscopic, kinetic, and thermodynamic studies using a variety of techniques [6,7,9–11]. Isothermal titration calorimetry (ITC) is one such technique that has been used to investigate the thermodynamic driving forces that govern metal binding in biological systems [12], specifically for the Ca^{2+}-cTnC system [13,14]. ITC experimentally measures the flow of heat upon addition of a titrant to a titrand. Heat is inherently non-selective in nature and, consequently, inclusive of all chemical processes occurring in the reaction cell. Thus, ITC is an ideal technique to study metal-protein interactions because it is not restricted by the spectroscopic properties (or lack thereof) of the metal. However, experimental systems that involve metal ions require special attention due to their complex solution chemistry. Metal chemistry includes, but is not limited to, undesired interactions such as precipitation, hydrolysis, redox, in addition to other intrinsically coupled equilibria in such as metal–buffer interactions and de/protonation of the buffer and/or ligand [15–17] Scheme 1 represents the most common coupled equilibria present when divalent metals bind to ligands.

The bulk thermodynamic technique of ITC measures the net sum of these equilibria, Eq. (1), in a single titration experiment.

$$\Delta H_{ITC} = \Delta H_{ML} - (n)\Delta H_{HL} + (n)\Delta H_{HB} - r\Delta H_{MB} \tag{1}$$

In this equation, n represents the number of protons displaced upon metal binding to the ligand and r is the fraction of metal bound to buffer at a specific experimental pH. The desired metal-ligand (ΔH_{ML}) or metal-buffer (ΔH_{MB}) contributions to the net enthalpy (ΔH_{ITC}) can be determined if all other equilibria are known by simply rearranging Eq. (1).

$$Metal^{n+} + Ligand \rightleftharpoons [Metal\text{-}Ligand]^{n+} \qquad \Delta H_{ML}$$

$$[Ligand\text{-}H] \rightleftharpoons [Ligand]^{-} + H^{+} \qquad \Delta H_{HL}$$

$$Buffer + H^{+} \rightleftharpoons [Buffer\text{-}H]^{+} \qquad \Delta H_{HB}$$

$$[Metal\text{-}Buffer]^{n+} \rightleftharpoons Metal^{n+} + Buffer \qquad \Delta H_{MB}$$

Scheme 1. Examples of equilibria associated with divalent metal ion binding to a simple ligand along with ΔH designations for each.

While Hess's law allows for the determination of ΔH_{MB} and ΔH_{ML} from enthalpies reported in the literature, converting known equilibrium constants to ΔG and employing the same method will not generate the correct condition independent equilibria values. This is due to the way that the equilibrium constant (K_{ITC}) is defined in fitting algorithms for ITC data; a more thorough discussion is available in previous studies [16]. Fortunately, the methods developed to address this concern involve the same equilibrium expressions presented in Scheme 1.

Herein, we report the extraction of metal-buffer enthalpy and binding parameters from Ca^{2+}-EDTA titrations. These data were, in turn, used to determine buffer-independent and buffer/pH- adjusted thermodynamic parameters for Ca^{2+}-binding to human cardiac troponin C (hcTnC) and the N-domain of the protein, respectively, under identical conditions of buffer and ionic strength. This process can be readily extended to the binding of other metals to hcTnC and other EF-hand containing proteins.

2. Experimental

2.1. Materials

EDTA used to determine metal-buffer parameters was purchased from Sigma and MP Biomedical, respectively. Both cadmium and calcium atomic absorption standards (1000 ppm, 3% HCl) were purchased from Ricca Chemicals. Ultra-Pure grade Bis-Tris buffer was purchased from VWR (Amresco), while MES and MOPS buffers were purchased from Sigma at ≥99.5 purity. Recombinant pET3d plasmid coding for protein hcTnC was generously donated by the Chalovich laboratory (Biochemistry and Molecular Biology Program at the Brody School of Medicine). Isopropyl β-D-thiogalactopyranoside (IPTG) was purchased from IBI Scientific and used to induce protein expression. Phenyl Sepharose CL-4B used for hydrophobic column chromatography was purchased from GE Healthcare. All protein, ligand, and buffer solutions were prepared using 18 MΩ water. To avoid metal contamination, all glassware used for solution preparation was acid washed and thoroughly rinsed with 18 MΩ water.

2.2. Preparation of metal and EDTA stocks

All Ca^{2+} stock solutions (~5 mM) were prepared from atomic absorption standards in 50 mM buffer (Bis-Tris, MES, or MOPS), 100 mM KCl, and brought to a pH of 7.0. Three EDTA stock solutions (0.5 mM) in each of the above buffer conditions were likewise prepared. Respective buffer solutions containing 50 mM buffer, 100 mM KCl at $pH = 7.0$ were prepared and used to dilute the above metal and ligand stocks.

A series of 1 mM metal solutions was prepared for the EDTA titrations by dilution of the 5 mM stock with the respective buffer solution. EDTA solutions (0.1 mM) were prepared in a similar manner to minimize the heat of dilution, ΔH_{dil}. All metal stock solutions were analyzed by ICP-OES at RTI International to determine precise concentrations.

2.3. Preparation of hcTnC protein and metal solutions

Recombinant pET3d plasmid coding for hcTnC was transformed into BL21 Star™ (DE3) cells and the protein was over-expressed and purified as described previously [18]. Protein samples were flash frozen and stored at −80 °C until experimentation. To ensure that the protein stock was free of metal ion, hcTnC was dialyzed against 20 mM EDTA, 50 mM buffer (Bis-Tris, MES, or MOPS) at $pH = 7.0$, and 100 mM KCl solution in BioDesignDialysis™ dialysis tubing (28.7 mm wet diameter, 3500 MWCO) 3× in ≥10× the protein solution volume. To remove EDTA, the protein stock was then exhaustively dialyzed against the respective buffer solution with no EDTA present (3 to 4× in ≥10× the protein solution volume) [19]. Protein concentrations were calculated by measuring the absorbance at 280 nm ($\varepsilon_{280} = 4470\ M^{-1} \cdot cm^{-1}$) [20].

ITC protein samples (~20–100 μM, 2.5 mL) and metal solution (1.5 to 2 mM) were prepared by dilution with the respective buffer. All protein-metal solutions were analyzed by ICP-OES to determine precise concentration of metal. The *pH* of metal, protein, and EDTA solutions were confirmed using an Orion *pH* probe and VWR *pH* meter.

2.4. Isothermal titration calorimetry

All ITC measurements were carried out at 25 °C on a MicroCal VP-ITC ultrasensitive titration calorimeter. Titrations were run in triplicate or quadruplet to ensure reproducibility and allow for statistical analysis. The metal (titrant) and ligand or protein (titrand) stocks were diluted with identical buffer to a final titrant concentration of 1 to 1.5 mM and titrand concentration of 20 to 100 μM as described previously. The titrand in the reaction cell was stirred at 307 rpm to ensure rapid mixing. In a typical experiment, 8 μL of titrant was delivered to the reaction cell over 20 s with a 350 s interval between injections to allow complete equilibration. Titrations continued until 3 to 5 M equivalents of metal were added to ensure complete saturation of the peptide. A background titration consisting of the identical titrant solution but only the buffer solution in the sample cell was run for each reaction to assure that unaccounted equilibria was not present (data not shown). The last ten data points were averaged, and that heat subtracted from each experimental titration to account for the heat of dilution.

ITC data are presented with the raw data (power vs. time) on the top panel, where each peak represents an injection of titrant into the reaction cell, and the integrated and normalized heat plotted vs. the molar ratio of titrant to titrand on the bottom panel. The data were subsequently analyzed with either a “Single Set of Identical Sites” binding model (EDTA titrations) or “Sequential Binding Sites” model (hcTnC titrations) by the Origin 7.0 software package supplied by MicroCal.

3. Results and discussion

3.1. Extraction of Ca^{2+}-buffer binding parameters from Ca^{2+}-EDTA titrations

ITC data were collected for Ca^{2+} binding to EDTA in three different buffers (Scheme 2) with identical values of concentration, *pH*, and ionic strength. Representative binding isotherms for the titration of Ca^{2+} into EDTA in Bis-Tris, MES, and MOPS buffers (Fig. 2A) reveal a single exothermic event at $n = 1$ and were fit to a “Single Set of Identical Sites” model (Table 1). The enthalpy values obtained for the different buffer systems differ by ~1.4 to 3 kcal/mol indicating a significant contribution to ΔH_{ITC} from buffer-dependent equilibria. To extract buffer-independent parameters, one must account for these additional equilibria in the system (Scheme 1). Fortunately, many of these equilibria such as pK_a values and ionization enthalpies for various buffers and chelating ligands are known and reported in the literature [21]. This allows one to extract buffer-independent binding constants using the following equations and enthalpies using Hess's law.

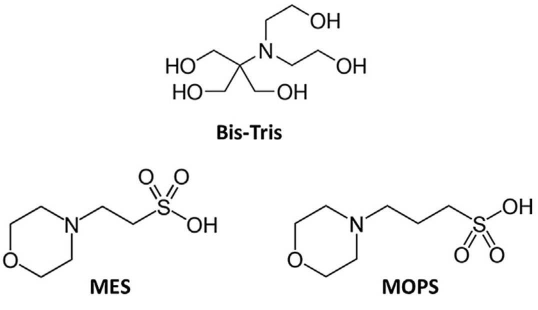

Scheme 2. Chemical structures of 2-Bis(2-hydroxyethyl)amino-2-(hydroxymethyl)-1,3-propanediol (Bis-Tris), 2-morpholinoethanesulfonic acid (MES), and 3-(N-morpholino) propanesulfonic acid (MOPS).

The subsequent expressions were derived from equilibria listed in Table 2 and show the relationship between K_{ML} and K_{ITC} [16]. It is important to note that a $CaHEDTA^{-1}$ complex has been observed, and a Log K = 3.18 has been reported in NIST [21]. However, at pH 7, 99.999% of the Ca^{2+} is present as a $CaEDTA^{2-}$ complex, while the $CaHEDTA^{-}$ is only ~0.001% abundant. Consequently, we chose to ignore the contributions of $CaHEDTA^{-}$ in equilibrium and enthalpy calculations.

Eq. (3) assumes a diprotic ligand because the four carboxylic acids of EDTA have *pKa* values well below the experimental *pH*. It can, however, be extended to account for any number ionizable protons. In addition, Eq. (4) assumes a single metal-buffer species and can be extended to account for additional species if present and Log K_{MB} are known. However, one major strength of our approach is that many of the “apparent” metal buffer constants (K_{MB}) can be determined under identical experimental conditions. This “apparent” affinity is directly applicable to other experiments carried out under identical conditions and all speciation involving interactions between the metal and buffer are inherently incorporated into this value; the same is true for ΔH.

$$K_{ML} = K_{ITC} \times R \times Q \tag{2}$$

where

$$Q = 1 + K_{HL}[H^+] + \beta_{H_2L}[H^+]^2 \tag{3}$$

and

$$R = 1 + K_{MB}[B] \tag{4}$$

Substituting *R* into Eq. (2) allows us to solve for K_{MB}. All variables in Eq. (5) are experimentally determined (K_{ITC}), readily available in the literature ($K_{ML} = K_{CaEDTA}$, K_{HL}, K_{H_2L}), or calculated from literature values (Q, β_{H_2L}) (Table 2).

$$K_{MB} = \frac{K_{ML}}{K_{ITC}Q[B]} - \frac{1}{[B]} \tag{5}$$

The desired ΔH_{MB} can be determined from the known ionization enthalpies and *pKa* values of EDTA and the respective buffers used in the above Ca^{2+} titrations, and by rearranging ΔH_{ITC} expression shown in Table 2.

$$\Delta H_{MB} = (\Delta H_{ML} - (a+b)\Delta H_{HL} - b\Delta H_{H_2L} + (a+2b)\Delta H_{HB} - \Delta H_{ITC})/r \tag{6}$$

Eq. (6) is an extended version of Eq. (1) that considers the relevant speciation that is occurring in this experiment. The coefficients, *a, b*, and *r* represent the fraction of both protonated EDTA and Ca^{2+}-buffer species in solution respectively and can be calculated from the K_{eq} expressions found in Table 2. The expression $a + 2b$ found in Eq. (6) represents the total number of protons exchanged upon Ca^{2+} binding to EDTA and is easily calculated from the *pH* of the solution and *pKa* values of the ionizable protons of the ligand (Eqs. (7) and (8)).

$$a = \frac{[HL]}{[L]_{Total}} = \frac{K_{HL}[H^+]}{1 + K_{HL}[H^+] + \beta_{H_2L}[H^+]^2} = \frac{K_{HL}[H^+]}{Q} \tag{7}$$

$$b = \frac{[H_2L]}{[L]_{Total}} = \frac{\beta_{H_2L}[H^+]^2}{1 + K_{HL}[H^+] + \beta_{H_2L}[H^+]^2} = \frac{\beta_{H_2L}[H^+]^2}{Q} \tag{8}$$

$$r = \frac{[MB]}{[M]_{Total}} = \frac{K_{MB}[B]}{1 + K_{MB}[B]} = \frac{K_{MB}[B]}{R} \tag{9}$$

Calculated K_{MB} and ΔH_{MB} values are listed in Table 3. The Log K_{MB} of 2.4 value derived for Bis-Tris agrees quite well with the NIST value of 2.25 [21]. Calcium's interaction with Bis-Tris also appears to be more stable than MES (Log K_{MB} = 1.6) and MOPS (Log K_{MB} = 2.1) This is not surprising as the ionic radii of the Ca^{2+} ion (0.99 Å) is optimal for

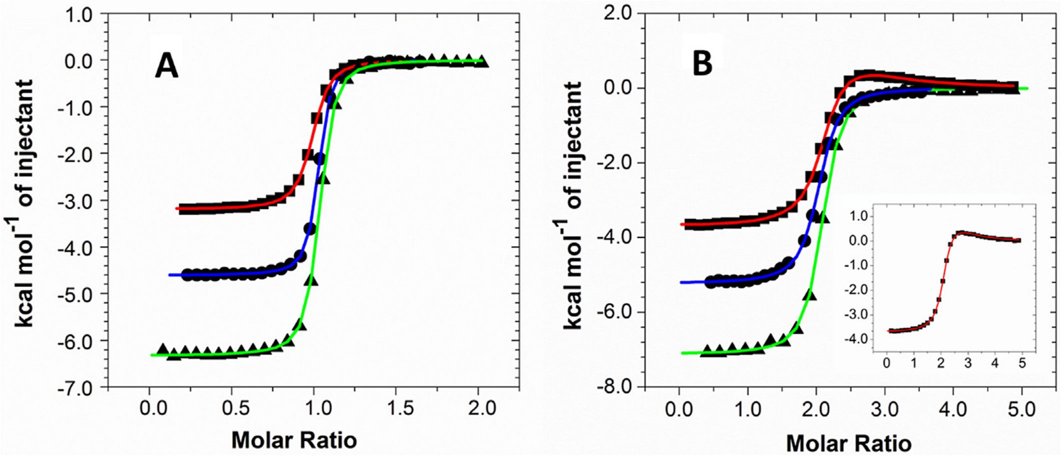

Fig. 2. A) Representative ITC data of Ca^{2+} titrated into EDTA in Bis-Tris (■), MES (▲), and MOPS (●) buffer at 25 °C. B) Representative ITC data of Ca^{2+} titrated into apo hcTnC in Bis-Tris (■), MES (▲), and MOPS (●) buffer at 25 °C. The inset depicts the Ca^{2+} titration in Bis-Tris buffer to more distinctly highlight the endothermic binding event at $n = 3$. All samples were in 50 mM buffer, $pH = 7.0$, and 100 mM KCl. Thermodynamic data are listed in Tables 3 and 4.

Table 1
Buffer ionization logarithmic binding constants and enthalpies from NIST database [21].

Buffer systems[a]	Log K_{HB}	ΔH_{HB} (kcal/mol)
Bis-Tris	6.54 (± 3)	−6.86
MES	6.24	−3.54 (± 3)
MOPS	7.184 (± 1)	−5.01 (± 1)

[a] Data reported for the following conditions: 0.0 M ionic strength and 25 °C (MES and MOPS) and 0.1 M ionic strength and 25 °C (Bis-Tris).

chelation by Bis-Tris, allowing for maximal hydroxyl group coordination and a favorable hard-soft acid-base (HSAB) interaction [22,23]. When comparing the morpholine buffers, the Ca^{2+} interaction with MOPS appears to be more stable than MES. Although a tertiary amine is not an ideal ligand for Ca^{2+} due to a mismatch in HSAB properties, the borderline base has been made harder due to the presence of the oxygen in the morpholine ring. However, the amine present in MES is more acidic and possibly less nucleophilic than its MOPS counterpart, most likely due to the shorter sulfonate linkage. This may contribute to the weaker interaction between MES and Ca^{2+}.

The Ca^{2+} buffer enthalpies were determined to be −5.8 (± 0.4), −0.2 (± 0.6), and 0.1 (± 0.4) kcal/mol for Bis-Tris, MES, and MOPS respectively. The Ca^{2+}-Bis-Tris interaction is the most favorable and correlates with the more favorable Ca^{2+}-hydroxyl bonds. The enthalpies for the MES and MOPS were observed to be small in magnitude and statistically the same. The small enthalpies reflect the weak bonding interactions between Ca^{2+} and the morpholine buffers.

We utilized the linear relationship between experimental heats and buffer ionization enthalpies to determine the number of protons exchanged upon Ca^{2+} binding to EDTA [15,24]. This was accomplished by first subtracting the respective Ca^{2+}-buffer enthalpies (Table 3) from ΔH_{ITC} values obtained from Ca^{2+}-EDTA titrations (Table 3) and plotting these values versus known buffer ionization enthalpies (Table 1). The experimental value of 1.12 (± 0.05) was obtained from the slope of the graph generated in Fig. 3A and agrees very well with 1.13, the theoretical number of protons released/exchanged upon Ca^{2+}-EDTA binding. Taken together, these results provide us with confidence in our experimental data and data analysis method. The K_{MB} and ΔH_{MB} values were thus used to extract buffer and or pH-adjusted binding parameters for the reaction between Ca^{2+} and hcTnC.

Table 2
Depiction of the individual equilibria that contribute to the binding constant and enthalpy measured in the ITC reaction cell (K_{ITC} and ΔH_{ITC}) when titrating Ca^{2+} into EDTA in a buffer system, B.[a]

Equilibria	EDTA	K_{Eq}	ΔH	n[d]
Individual	$M^{2+} + EDTA^{4-} \rightleftharpoons M\text{-}EDTA^{2-}$	$K_{ML} = \frac{[ML]}{[M][L]}$[b]	ΔH_{ML}[c]	1
	$EDTAH^{3-} \rightleftharpoons EDTA^{4-} + H^+$	$\frac{1}{K_{HL}} = \frac{[H^+][L]}{[HL]}$[b]	$-\Delta H_{HL}$[c]	$a + b$
	$EDTAH_2^{2-} \rightleftharpoons EDTAH^{3-} + H^+$	$\frac{1}{K_{H_2L}} = \frac{[H^+][HL]}{[H_2L]}$[b]	$-\Delta H_{H_2L}$[c]	b
	$B + H^+ \rightleftharpoons BH^+$	$K_{HB} = \frac{[HB]}{[H^+][B]}$[e]	ΔH_{HB}[e]	$a + 2b$
	$MB^{2+} \rightleftharpoons M^{2+} + B$	$\frac{1}{K_{MB}} = \frac{[M][B]}{[MB]}$[f]	$-\Delta H_{MB}$[f]	r
Sum reaction cell	$(1 - r)M^{2+} + rMB^{2+} + (1 - a - b)EDTA^{4-} + aEDTAH^{3-} + bEDTAH_2^{2-} \rightleftharpoons M\text{-}EDTA^{2-} + (a + b)BH^+$			
ΔH_{ITC}	$\Delta H_{ML} - (a + b)\Delta H_{HL} - b\Delta H_{H_2L} + (a + 2b)\Delta H_{HB} - r\Delta H_{MB}$			

[a] B represents 50 mM Bis-Tris, MES, or MOPS ($pH = 7.0$).

[b] Log $K_{ML} = 10.7$, Log $K_{HL} = 10.2$, Log $K_{H2L} = 6.1$. Values obtained from NIST database [21].

[c] $\Delta H_{ML} = -6.1$, $\Delta H_{HL} = -5.6$, $\Delta H_{H2L} = -4.2$. Values obtained from NIST database [21].

[d] Coefficients associated with listed equilibria.

[e] K_{HB} and ΔH_{HB} can be found in Table 1.

[f] K_{MB} and ΔH_{MB} were determined in this study (Table 3).

Table 3
Average best fit thermodynamic parameters (K_{ITC} and ΔH_{ITC}) and extracted thermodynamic parameters (K_{MB}, ΔH_{MB}, and Log K_{MB}) for Ca^{2+} binding to EDTA in various buffers.[a,b]

Buffer	K_{ITC} ($\times 10^6$)	ΔH_{ITC} (kcal/mol)	K_{MB} ($\times 10^2$)	ΔH_{MB} (kcal/mol)	Log K_{MB}
Bis-Tris	2.3 (± 0.1)	−3.08 (± 0.03)	2.7 (± 0.1)	−5.8 (± 0.4)	2.4
MES	9.5 (± 0.1)	−4.51 (± 0.02)	0.4 (± 0.1)	−0.2 (± 0.6)	1.7
MOPS	7.6 (± 0.4)	−6.37 (± 0.04)	1.2 (± 0.1)	0.1 (± 0.4)	2.1

[a] Data were fit utilizing a "Single set of Identical Sites" model and represent an average of at least four experiments. Data represent an average of ≥3 experimental repeats and are reported with the standard error of the mean.

[b] Data collected at 25 °C in 0.05 M buffer at a *pH* of 7.0 and 0.10 M KCl.

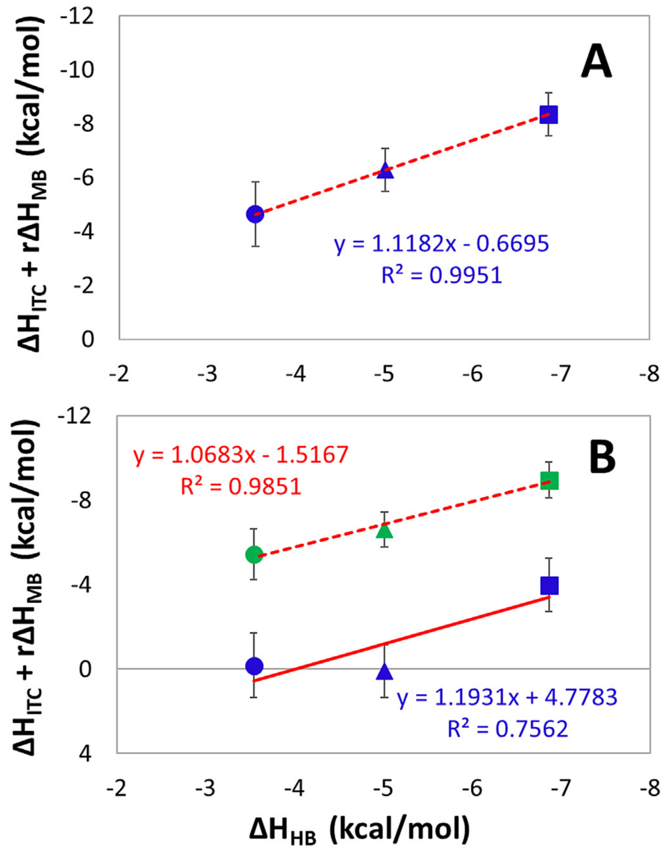

Fig. 3. Proton displacement plot (ΔH_{ITC} + r ΔH_{MB} versus $\Delta H_{ionization}$) for Ca^{2+} binding to A) EDTA and B) Ca^{2+} binding to the C-domain (green data marker, -----) and N-domain (blue data marker, ▬) of hcTnC in three buffers at 25 °C: (□) Bis-Tris, (○) MES, and (Δ) MOPS (50 mM buffer, *pH* = 7.0, and 100 mM KCl). The number of protons released upon metal binding were obtained from the slope of each graph. The error bars represent the 95% confidence intervals for each data point obtained from ≥3 experimental repeats.

3.2. Thermodynamic studies of Ca^{2+} binding to hcTnC in Bis-Tris, MES, and MOPS

ITC data were collected for Ca^{2+} binding to *apo*-hcTnC in the three buffers used in the EDTA experiment described above. Representative binding isotherms for the titration of Ca^{2+} into *apo*-hcTnC in Bis-Tris, MES, and MOPS buffers are shown in Fig. 2B. The thermogram collected in Bis-Tris (Fig. 2B inset) exhibits a strong exothermic binding event at a molar ratio of 2 and a second weaker and endothermic binding event at a molar ratio of 3. The thermogram is consistent with three metal ions binding to the full-length protein and displays a similar thermodynamic profile observed by Skowronsky et al., albeit under different buffer and ionic strength conditions (14). Interestingly, the endothermic feature was not observed in thermograms collected in MES or MOPS buffers; these data were fit to a "Single Set of Identical Sites" model. The lack of a quantifiable endothermic event appears to be consistent with the metal-buffer bond enthalpies reported in Table 3. The more negative and favorable the metal-buffer interaction, the greater net positive contribution to ΔH_{ITC}.

Bis-Tris data were fit to a "Sequential Binding Sites" model in the Origin software, constrained so that $K_1 = K_2$ and $H_1 = H_2$, indicating that the first two Ca^{2+} ions bind with positive cooperativity. This fit provides K_{ITC} values of 2.9 (± 0.4) × 10^6 and 4.3 (± 0.5) × 10^4 in addition to ΔH values of −3.7 (± 0.1) and 1.3 (± 0.1) kcal/mol (Table 4). The K_{ITC} values obtained are consistent with two high-affinity Ca^{2+} ions binding to the C-domain of hcTnC (with positive cooperativity) and a third low-affinity Ca^{2+} ion binding to the regulatory domain of the protein as seen in previous studies [13].

3.3. Extraction of buffer-independent binding parameters for Ca^{2+} binding to both the C-and N-domains of hcTnC

Coupled equilibria for Ca^{2+} binding to hcTnC are listed in Table 5. Determining buffer and *pH*-adjusted metal binding parameters requires a knowledge of the K_{MB} values obtained in the preceding EDTA titrations (Table 3), as well as the *pKa* values of the amino acid residues coordinated to Ca^{2+}. Ionizable amino acids are very sensitive to their chemical environment and their intrinsic *pKa*'s can vary by two or more units based on the microenvironment presented by the protein [25]. Determining these values often require a complex set of experiments [26,27], computational methods (vide infra), and knowledge of the protein structure. Although solution structures determined by NMR exist for Ca^{2+}-bound full hcTnC [10] and the N-domain of hcTnC in both the *apo*- and Ca^{2+}-bound forms [9], a structure for the *apo*-full length protein has not been reported. This is partly due to the large structural changes that occur upon Ca^{2+} ions binding to the C-domain of the protein [7,28].

While the lack of suitable *pKa* values for the C-domain prevented us from determining *pH*-adjusted data, proton competition should be identical in all buffers (due to the identical *pH*) with differences in K_{ITC} stemming from the competition of the metal-buffer complex only. We therefore chose to derive the buffer-independent values at *pH* = 7.0 for Ca^{2+} binding to both the C– and N-domain of the protein for comparison. Rearranging Eq. (5) and focusing solely on metal-buffer interactions, *R* (Eq. (4)), the following expression (Eq. (10)) was obtained and used to determine buffer-dependent K_{MP} for all three Ca^{2+} ions binding to hcTnC in Bis-Tris, MES, and MOPS buffers. These values can be found in Table 4.

$$K_{MP} = K_{ITC} \times (1 + K_{MB}[B]) \tag{10}$$

The K_{MP} values corresponding to binding of the first two Ca^{2+} ions are similar, therefore generating confidence in the data.

As formerly mentioned, the ΔH values that were determined from the ITC fits include contributions from several reactions that are coupled to Ca^{2+} binding to hcTnC; these include the dissociation of the metal-buffer complex as well as heats associated with proton flow from the protein to the buffer. To determine the buffer-independent enthalpy, one must determine the number of protons released upon Ca^{2+} binding to both the C– and N- domains. In the absence of protein *pKa*

Table 4

Best fit K_{ITC}, $\Delta H_{ITC,}$ and *buffer-independent* thermodynamic parameters (*K*, *ΔG*, *ΔH*, and *TΔS*) for Ca^{2+} binding to apo-hcTnC in various buffers.[a]

Parameter	Bis-Tris[b]	MES	MOPS	Average
$K_{ITC\ (1=2)}$	2.9 (± 0.4) × 10^6	2.0 (± 0.3) × 10^6	4.1 (± 0.5) × 10^6	NA[c]
$\Delta H_{ITC\ (1=2)}$	−3.7 (± 0.1)	−5.3 (± 0.1)	−6.7 (± 0.1)	NA[c]
$K_1 = K_2$	3.2 (± 0.4) × 10^7	5.4 (± 0.8) × 10^6	1.4 (± 0.2) × 10^7	1.7 (± 0.3) × 10^7
$\Delta G_{(1=2)}$	−10.4 (± 0.1)	−9.19 (± 0.1)	−9.74 (± 0.1)	−9.8 (± 0.1)
$\Delta H_{(1=2)}$	−1.4 (± 0.6)	−1.6 (± 0.6)	−1.2 (± 0.6)	−1 (± 1)
$T\Delta S_{(1=2)}$	8.6 (± 0.6)	7.6 (± 0.6)	8.5 (± 0.6)	8 (± 1)
$K_{ITC\ (3)}$	4.3 (± 0.5) × 10^4	NTD[d]	NTD[d]	NA[c]
$\Delta H_{ITC\ (3)}$	1.3 (± 0.1)	NTD[d]	NTD[d]	NA[c]
$K_{(3)}$	4.7 (± 0.6) × 10^5	–	–	4.7 (± 0.6) × 10^5
$\Delta G_{(3)}$	−7.7 (± 0.1)	–	–	−7.7 (± 0.1)
$\Delta H_{(3)}$	4.3 (± 0.4)	4.1 (± 0.6)	6.1 (± 0.6)	4.8 (± 0.8)
$T\Delta S_{(3)}$	11.9 (± 0.4)	–	–	11.9 (± 0.4)

Thermodynamic parameters are reported in kcal/mol.

[a] Data were collected at 25 °C in 0.050 M buffer at a *pH* of 7.0 and ionic strength of 0.10 M. Data represent an average of ≥ 3 experimental repeats and are reported with the standard error of the mean.

[b] Data were fit using a "Sequential Binding Sites" model.

[c] Data represent buffer specific data therefore "Average" is not applicable (NA).

[d] No thermal detection (NTD).

Table 5

Depiction of the additive equilibria that contribute to K_{eq} and *ΔH* measured in the ITC reaction cell (K_{ITC} and ΔH_{ITC}) when titrating Ca^{2+} into hcTnC in a buffer system, B.[a]

Equilibria	hcTnC	K_{eq}	Enthalpy	*n*
Individual	$M^{2+} + P \rightleftharpoons MP^{2+}$	$K_{MP} = \frac{[MP]}{[M][P]}$	ΔH_{MP}	1
	$PH^+ \rightleftharpoons P + H^+$	$\frac{1}{K_{HP}} = \frac{[H^+][P]}{[HP]}$	$-\Delta H_{HP}$	n_{H^+}[b]
	$B + H^+ \rightleftharpoons BH^+$	$K_{HB} = \frac{[HB]}{[H^+][B]}$	ΔH_{HB}	n_{H^+}[b]
	$MB^{2+} \rightleftharpoons M^{2+} + B$	$\frac{1}{K_{MB}} = \frac{[M][B]}{[MB]}$	$-\Delta H_{MB}$	*r*[c]
Sum reaction cell	$(1 - r)M^{2+} + rMB^{2+} + (1 - n_{H^+})P + n_{H^+}PH^+ \rightleftharpoons MP^{2+} + n_{H^+}BH^+$			

[a] B represents 50 mM Bis-Tris, MES, or MOPS (*pH* = 7.0).

[b] The slope of the lines depicted in Fig. 3B are equivalent to the value for n_{H^+} for the distinct C– and N-domain binding events.

[c] The calculation of *r* is described by Eq. (9).

values, we utilized the same experimental approach discussed above to determine the number of protons exchanged upon metal-protein binding [15,24]. Respective Ca^{2+}-buffer enthalpies (Table 3) were subtracted from ΔH_{ITC} values obtained from Ca^{2+}-hcTnC titrations (Table 4) and plotted versus known buffer ionization enthalpies listed in Table 1. The number of protons displaced upon Ca^{2+} binding to the C– and N-domain of hcTnC, as revealed in the slopes of the graphs generated in Fig. 3B, are 1.07 (± 0.05) and 1.2 (± 0.1) respectively.

These values differ significantly from those reported in a 2013 publication [14]. In that study, it was assumed that the metal buffer contributions (*ΔH* and K_{MB}) were negligible for the buffers used and this resulted in 0.5 ± 0.1 and 0.6 ± 0.2 protons displaced upon Ca^{2+} binding to the C– and N-domain's respectively. This discrepancy highlights the importance of accounting for metal-buffer interactions in all quantitative binding experiments where multiple buffers are used.

The ΔH_{MB} values determined in this study were used in the following equation to obtain ΔH_{MP}, where a positive slope or *n* value indicates the number of protons released upon metal binding and a negative *n* represents the number of protons captured by the metal-protein complex.

$$\Delta H_{MP} = \Delta H_{ITC} - (n)\Delta H_{HB} + r\Delta H_{MB} \tag{11}$$

The consistency in ΔH_{MP} for Ca^{2+} binding to the C-domain determined in multiple buffers provides confidence in the outlined method.

Taken together, these data suggest that metal-buffer interactions are considerable and contribute significantly to the observed binding affinities and enthalpies. We chose to provide evidence for this statement by collecting ITC data for Ca^{2+} binding to apo-hcTnC at 25 mM, 50 mM, and 100 mM Bis-Tris buffer concentrations (100 mM KCl and pH = 7.0; Supplementary Material Fig. S1). These data reveal a buffer-concentration dependence, with weaker "apparent" affinities and less favorable enthalpies occurring at higher buffer concentrations for the two high-affinity Ca^{2+} ions binding to the C-domain. The apparent affinities differed by factors of 0.55 and 0.29 derived from our buffer correction factors, *R* (Eq. (4)), providing additional confidence in our method (Supplementary Material). The low affinity Ca^{2+} data also appears to become weaker at higher buffer concentration, however additional replicates are required as these values tend to be subject to more error (Supplementary Material Fig. S1; Tables T3 and T4).

Correcting both the high affinity K_{ITC} and ΔH_{ITC} for metal-buffer interactions (Eqs. (10) and (11) respectively) resulted in K_{MP} and H_{MP} values that agree quite well and are within experimental error (Supplementary Material Table T1 and T2). This internal consistency in buffer-corrected binding parameters refutes the formation of ternary species [29].

3.4. Extraction of buffer and pH-adjusted enthalpy values for Ca^{2+} binding to the N-domain of hcTnC in Bis-Tris buffer

Obtaining *pH*-adjusted thermodynamic parameters requires knowledge of the *pKa* values and ionization enthalpies of the coordinating residues. A convenient alternative to experimentally determining *pKa* values of ionizable sidechains in proteins is to employ computational methods that require structural coordinates obtained from solution NMR or x-ray crystallography [30–33]. The solution structures of the N-terminal domain of hcTnC in both the apo- and Ca^{2+}-bound forms have been solved, revealing very little difference between the two structures [9]. We therefore chose to use the open access software, H++ [34], and the solution structures of both the Ca^{2+}-bound and *apo*-N-terminal domain (PDB ID 1AP4 and 1SPY respectively) to estimate the *pKa* values of all ionizable amino acid residues located in EF-hand loop II of the N-domain upon metal coordination (Supplementary Material Table T5).

The theoretical number of protons exchanged upon Ca^{2+} ion coordination is simply the sum of the change in fractional protonation states, Δf_{HA}, of each ionizable residues in the protein (Eqs. (12) and (13)).

$$\Delta f_{HA} = \sum (f_{HA_{Ca^{2+}}} - f_{HA_{apo}}) \tag{12}$$

where

$$f_{HA} = \frac{1}{1 + 10^{pH-pKa}} \tag{13}$$

The theoretical number of protons exchanged upon metal binding were calculated to be 1.92 at $pH = 7.0$, which is comparable to 1.2 (± 0.5) protons exchanged experimentally.

The primary coordination sphere of Ca^{2+} is fulfilled by amino acids located at positions 1, 3, 5, 7, 9, and 12 of EF-hand Loop II (Fig. 1B). Asp-65, Asp-67 (positions 1 and 3 respectively) and Glu-76 (position 12) provide monodentate coordination through their respective carboxylate side-chains while Glu-76 coordinates in a bidentate fashion. Ser-69 coordinates via its hydroxyl side-chain and Thr-71 binds via its carbonyl backbone. Coordination is made complete by a water molecule bridged by Asp-73 [6,10]. The program calculated *pKa* values of 8.4, 5.0, and 10.8 for the coordinating residues Asp-65, Asp-67, and Glu-76 respectively. For the apo-structure, the *pKa* values were found to be 5.5, 6.3, and 8.3 for the Asp-65, Asp-67, and Glu-76 residues respectively (Supplementary Material Table T5). Ser-69 completes the Ca^{2+} pentagonal bipyramidal coordination; however, a *pKa* for this amino acid was not provided by the H+ + program [30]. Furthermore, Ca^{2+} is a moderate Lewis acid and not able to displace the hydroxyl proton on serine [35].

Calculating the sum of the change in fractional protonation at just the coordinating amino acids resulted in a net 0.83 displacement in protons upon Ca^{2+} binding (Table 6). This value indicates that 43% of the proton flow that occurs upon Ca^{2+} binding is localized at the metal coordinating residues.

Armed with the theoretical fraction of protons exchanged upon metal binding for each ionizable amino acid and their estimated ionization enthalpies obtained from the NIST database [21], we calculated a net protonation enthalpy, $n\Delta H_{HP}$, of −2.32 kcal/mol and an ΔH_{HP} of −1.21 kcal/mol assuming an n of 1.92 as calculated by the H+ + program (Supplementary Material Table T6). The buffer and *pH*-adjusted K_{MP} and ΔH_{MP} were determined from Eqs. (14) and (15), using the experimentally determined n value of 1.2, and found to be 1.3 (± 0.2) × 10^7 and 2.8 (± 0.7) kcal/mol respectively.

$$K_{MP} = K_{ITC} \times (1 + K_{MB}[B]) \times (1 + K_{HP}[H^{+}]) \tag{14}$$

$$\Delta H_{MP} = \Delta H_{ITC} - (n)\Delta H_{HB} + (n)\Delta H_{HP} + (r)\Delta H_{MB} \tag{15}$$

The enthalpy of binding to the N-domain differs from the values reported by Skowronsky et al. (−2.1 kcal/mol) by a difference of 4.86 kcal/mol due to incorrectly accounting for metal-buffer interactions and protonation enthalpies for coordinating amino acids. The positive endothermic contribution to Gibbs free energy indicates that metal binding to the N-domain of hcTnC under aqueous conditions and close to physiological ionic strength is entropically driven ($T\Delta S = 12.5$ kcal/mol). It is known that metal binding to the N-domain of hcTnC does not result in a significant exposure of hydrophobic residues [9]; consequently, the typical decrease in entropy as water molecules form highly rigid and structured clathrate structures surrounding hydrophobic residues does not occur in our system. The favorable entropy change may result from the positive entropic contribution provided by desolvation of the Ca^{2+} ion upon binding to the protein.

4. Conclusions

In this study, we applied a procedure developed by Grossoehme and coworkers [16] to determine the metal buffer-independent binding parameters of Ca^{2+} binding to hcTnC, an EF-hand protein required for cardiac muscle contraction. Metal-buffer binding constants and enthalpies, previously missing from the literature, were extracted from EDTA titrations and used to determine metal-buffer parameters for metal-protein interactions. By accounting for metal-buffer interactions, the experimental number of protons released from the N-domain was quantified and lies within error of the theoretical value. This allowed us to determine both buffer and *pH*-adjusted thermodynamic parameters for Ca^{2+} binding to the N-domain of hcTnC, the region of the protein responsible for sensing Ca^{2+} and initiating cardiac muscle contraction. This study reveals the importance of considering both metal-buffer and proton displacement equilibria when reporting condition-independent thermodynamic values. Most importantly, this method can be used to directly compare the binding thermodynamics of a variety of metal ions to biomolecules in the absence of convoluting metal-buffer interactions. We plan to further investigate essential and toxic metal interactions with hcTnC to probe binding specificity and identify heavy metal interactions that may be linked to harmful health effects.

Notes

The authors declare no competing financial interest.

Acknowledgment

The authors would like to thank James Harrington at RTI International for his help with metal concentration determination and use of their ICP-OES. Most importantly, the authors would like to thank

Table 6
Theoretical and experimental proton release of Ca^{2+} binding to the C– and N-domains of human cardiac troponin C[a] and buffer and *pH*-adjusted thermodynamic parameters (K, ΔG, ΔH, and $T\Delta S$) Ca^{2+} binding to the N-domain of apo-hcTnC.

Fractional protonation states and proton displacement						
Ca^{2+} Binding	Coordinating amino acid residues & net fractional protonation states				Proton displacement	
					Theoretical[a]	Experimental
C-Domain loop III	*Asp105*	*Asn107*	*Asp109*	*Glu116*	NA	1.1 (± 0.1)
C-Domain loop IV	*Asp141*	*Asn143*	*Asp145*	*Glu152*		
N-Domain loop II	*Asp65*	*Asp67*	*Ser69*	*Glu76*	0.83 (1.92)[b]	1.2 (± 0.5)
	0.92	−1.4	NA	0.05		
Buffer and *pH*-adjusted binding parameters[c]						
Ca^{2+} Binding	$K_{(3)}$		$\Delta G_{(3)}$ (kcal/mol)		$\Delta H_{(3)}{}^{d}$ (kcal/mol)	$T\Delta S_{(3)}$ (kcal/mol)
N-Domain loop II	1.3 (± 0.2) × 10^7		−9.7 (± 0.1)		2.8 (± 0.7)	12.5 (± 0.7)

[a] The *pKa* values of metal coordinating amino acid side-chains present in the Ca^{2+} bound and apo solution structures were determined from the H^{++} database (http://biophysics.cs.vt.edu/H++) and utilized to determine the sum of the change in fractional protonation states of coordinating residues upon Ca^{2+} binding. Input structures: PDB 1AP4 and 1SPY for the Ca^{2+}-bound and apo-structures respectively.

[b] Sum of the change in fractional protonation states for all ionizable amino acid residues present in the Ca^{2+}-bound and apo solution structures.

[c] Data represent an average of ≥3 experimental repeats and are reported with the standard error of the mean.

Dr. Joseph M. Chalovich at the Brody School of Medicine for providing us with plasmids and for scientific advice and support, and Drs. Andy Sargent, Andrew Morehead and William Allen for their helpful discussions. The authors are grateful to East Carolina University's Undergraduate Research and Creativity Awards and the Department of Chemistry CURE Awards for partial funding of this project. This material is based upon work supported by the National Science Foundation under Grant No. CHE 1710347.

Appendix A. Supplementary data

Supplementary data to this article can be found online at https://doi.org/10.1016/j.bbapap.2019.01.004.

References

[1] K.L. Haas, K.J. Franz, Application of metal coordination chemistry to explore and manipulate cell biology, Chem. Rev. 109 (2009) 4921–4960, https://doi.org/10.1021/cr900134a.

[2] Z. Ma, F.E. Jacobsen, D.P. Giedroc, Coordination chemistry of bacterial metal transport and sensing, Chem. Rev. 109 (2009) 4644–4681, https://doi.org/10.1021/cr900077w.

[3] M. Yáñez, J. Gil-Longo, M. Campos-Toimil, Calcium binding proteins, in: M.S. Islam (Ed.), Calcium Signaling, vol. 740, Springer Netherlands, Dordrecht, 2012, pp. 461–482.

[4] M.C. Schaub, C.W. Heizmann, Calcium, troponin, calmodulin, S100 proteins: from myocardial basics to new therapeutic strategies, Biochem. Biophys. Res. Commun. 369 (2008) 247–264.

[5] R.D. Burgoyne, Neuronal calcium sensor proteins: generating diversity in neuronal Ca^{2+} signalling, Nat. Rev. Neurosci. 8 (2007) 182–193 (DOI: nrn2093 [pii).

[6] J.L. Gifford, M.P. Walsh, H.J. Vogel, Structures and metal-ion-binding properties of the Ca^{2+}-binding helix-loop-helix EF-hand motifs, Biochem. J. 405 (2007) 199–221.

[7] S. Takeda, A. Yamashita, K. Maeda, Y. Maeda, Structure of the core domain of human cardiac troponin in the Ca(II)-saturated form, Nature 424 (2003) 35–41, https://doi.org/10.1038/nature01780.

[8] O. Teleman, T. Drakenberg, S. Forsen, E. Thulin, Calcium and cadmium binding to troponin C. Evidence for cooperativity, Eur. J. Biochem. 134 (1983) 453–457.

[9] L. Spyracopoulos, M.X. Li, S.K. Sia, S.M. Gagne, M. Chandra, R.J. Solaro, B.D. Sykes, Calcium-induced structural transition in the regulatory domain of human cardiac troponin C, Biochemistry 36 (1997) 12138–12146.

[10] Samuel K. Sia, Monica X. Li, Leo Spyracopoulos, Stéphane M. Gagné, Wen Liu, John A. Putkey, D. Brian, Sykes Structure of Cardiac Muscle Troponin C Unexpectedly reveals a Closed Regulatory Domain, J. Biol. Chem. 272 (1997) 18216–18221, https://doi.org/10.1074/jbc.272.29.18216.

[11] K. Yamada, Calcium binding to troponin C as a primary step of the regulation of contraction. A microcalorimetric approach, Adv. Exp. Med. Biol. 538 (2003) 203–212.

[12] D.E. Wilcox, Isothermal titration calorimetry of metal ions binding to proteins: an overview of recent studies, Inorg. Chim. Acta 361 (2008) 857–867, https://doi.org/10.1016/j.ica.2007.10.032.

[13] K. Kometani, K. Enthalpy Yamada, Entropy and heat capacity changes induced by binding of calcium ions to cardiac troponin C, Biochem. Biophys. Res. Commun. 114 (1983) 162–167, https://doi.org/10.1016/0006-291X(83)91608-X.

[14] R.A. Skowronsky, M. Schroeter, T. Baxley, Y. Li, J.M. Chalovich, A.M. Spuches, Thermodynamics and molecular dynamics simulations of calcium binding to the regulatory site of human cardiac troponin C: evidence for communication with the structural calcium binding sites, J. Biol. Inorg. Chem. 18 (2013) 49–58 DOI https://doi.org/10.1007/s00775-012-0948-2.

[15] N.E. Grossoehme, A.M. Spuches, D.E. Wilcox, Application of isothermal titration calorimetry in bioinorganic chemistry, J. Biol. Inorg. Chem. 15 (2010) 1183–1191 DOI https://doi.org/10.1007/s00775-010-0693-3.

[16] R.A. Johnson, O.M. Manley, A.M. Spuches, N.E. Grossoehme, Dissecting ITC data of metal ions binding to ligands and proteins, Biochim. Biophys. Acta 1860 (2016) 892–901 DOI https://doi.org/10.1016/j.bbagen.2015.08.018.

[17] C.F. Quinn, M.C. Carpenter, M.L. Croteau, D.E. Wilcox, Isothermal Titration Calorimetry Measurements of Metal Ions Binding to Proteins, Methods Enzymol. 567 (2016) 3–21 DOI https://doi.org/10.1016/bs.mie.2015.08.021.

[18] J.R. Pinto, M.S. Parvatiyar, M.A. Jones, J. Liang, M.J. Ackerman, J.D. Potter, A functional and structural study of troponin C mutations related to hypertrophic cardiomyopathy, J. Biol. Chem. 284 (2009) 19090–19100 DOI https://doi.org/10.1074/jbc.M109.007021.

[19] A. Mónico, E. Martínez-Senra, F.J. Cañada, S. Zorrilla, D. Pérez-Sala, Drawbacks of dialysis procedures for removal of EDTA, PLoS One 12 (2017) 1–9, https://doi.org/10.1371/journal.pone.0169843.

[20] Gill, S. C.; von Hippel, P. H. Calculation of protein extinction coefficients from amino acid sequence data. Anal. Biochem. 1989, 182, 319–26. DOI: https://doi.org/10.1016/0003-2697(89)90602–7.

[21] R.M. Smith, A.E. Martell, R.J. Motekaitis, NIST Standard Reference Database 46. Critically selected Stability Constants of Metal Complexes Database, (2004) (Version 8 for Windows).

[22] K.H. Scheller, T.H. Abel, P.E. Polanyi, P.K. Wenk, B.E. Fischer, H. Sigel, Metal ion/buffer interactions: Stability of binary and ternary complexes containing 2-[bis(2-hydroxyethyl)amino]-2(hydroxymethyl)-1,3-propanediol (Bis-tris) and adenosine 5′-triphosphate (ATP), Eur. J. Biochem. 107 (1980) 455.

[23] Sigel, H.; Scheller, K. H.; Prijs, B. Metal ion/buffer interactions Part III: Stability of alkali and alkaline earth ion complexes with triethanolamine (Tea), 2-amino-2(hydroxymethyl)-1,3-propanediol (tris)and 2-[bis(2-hydroxyethyl)-amino] 2(hydroxymethyl)-1,3-propanediol (Bis-tris) in aqueous and mixed solvents. Inorg. Chim. Acta 1982, 66, 147–155. DOI: https://doi.org/10.1016/S0020-1693(00)) 85805–3.

[24] M.L. Doyle, G. Louie, P.R. Dal Monte, T.D. Sokoloski, Tight binding affinities determined from thermodynamic linkage to protons by titration calorimetry, Methods in Enzymology, vol. 259, Elsevier Science & Technology, United States, 1995, pp. 183–194.

[25] C.N. Pace, G.R. Grimsley, J.M. Scholtz, Protein ionizable groups: pK values and their contribution to protein stability and solubility, J. Biol. Chem. 284 (2009) 13285–13289, https://doi.org/10.1074/jbc.R800080200.

[26] A.M. Rich, E. Bombarda, A.D. Schenk, P.E. Lee, E.H. Cox, A.M. Spuches, L.D. Hudson, B. Kieffer, D.E. Wilcox, Thermodynamics of Zn^{2+} binding to Cys2His2 and Cys2HisCys zinc fingers and a Cys4 transcription factor site, J. Am. Chem. Soc. 134 (2012) 10405–10418 (DOI: 10.1021/ja211417g [doi).

[27] A. Onufriev, D.A. Case, G.M. Ullmann, A novel view of pH titration in biomolecules, Biochemistry 40 (2001) 3413–3419, https://doi.org/10.1021/bi002740q.

[28] M.X. Li, M. Chandra, J.R. Pearlstone, K.I. Racher, G. Trigo-Gonzalez, T. Borgford, C.M. Kay, L.B. Smillie, Properties of isolated recombinant N and C domains of chicken troponin C, Biochemistry 33 (1994) 917–925, https://doi.org/10.1021/bi00170a010.

[29] C. Sacco, R.A. Skowronsky, S. Gade, J.M. Kenney, A.M. Spuches, Calorimetric investigation of copper(II) binding to Abeta peptides: thermodynamics of coordination plasticity, J. Biol. Inorg. Chem. 17 (2012) 531–541 DOI https://doi.org/10.1007/s00775-012-0874-3.

[30] R. Anandakrishnan, B. Aguilar, A.V. Onufriev, H++ 3.0: automating pK prediction and the preparation of biomolecular structures for atomistic molecular modeling and simulations, Nucleic Acids Res. 40 (2012) 537.

[31] D. Bashford, M. Karplus, pKa's of ionizable groups in proteins: atomic detail from a continuum electrostatic model, Biochemistry 29 (1990) 10219–10225.

[32] J.C. Gordon, J.B. Myers, T. Folta, V. Shoja, L.S. Heath, A. Onufriev, H++: a server for estimating pKas and adding missing hydrogens to macromolecules, Nucleic Acids Res. 33 (2005) 368.

[33] J. Myers, G. Grothaus, S. Narayanan, A. Onufriev, A simple clustering algorithm can be accurate enough for use in calculations of pKs in macromolecules, Proteins 63 (2006) 928–938 DOI https://doi.org/10.1002/prot.20922.

[34] H++. http://biophysics.cs.vt.edu/H++ (accessed October 2018).

[35] G. Berthon, Critical evaluation of the stability constants of metal complexes of amino acids with polar side chains, Technical Report, Pure Appl. Chem. 67 (1995) 1117–1240, https://doi.org/10.1351/pac199567071117.